

Article

ECMWF Ensemble Forecasts of Six Tropical Cyclones That Formed during a Long-Lasting Rossby Wave Breaking Event in the Western North Pacific

Russell L. Elsberry^{1,2,*}, Hsiao-Chung Tsai³ , Wei-Chia Chin⁴ and Timothy P. Marchok⁵ ¹ Lyda Hill Institute for Human Resilience, University of Colorado, Colorado Springs, CO 80918, USA² Department of Meteorology, Naval Postgraduate School, Monterey, CA 93944, USA³ Department of Water Resources and Environmental Engineering, Tamkang University, New Taipei City 291301, Taiwan⁴ Hsinchu Management Office, Irrigation Agency, Ministry of Agriculture, Zhubei City, Hsinchu County 302, Taiwan⁵ NOAA Geophysical Fluid Dynamics Laboratory, Princeton, NJ 08540, USA

* Correspondence: relsberr@uccs.edu

Abstract: The ECMWF's ensemble (ECEPS) predictions are documented for the lifecycles of six tropical cyclones (TCs) that formed during a long-lasting Rossby wave breaking event in the western North Pacific. All six TC tracks started between 20° N and 25° N, and between 136° E and 160° E. All five typhoons recurved north of 30° N, and the three typhoons that did not make landfall had long tracks to 50° N and beyond. The ECEPS weighted mean vector motion track forecasts from pre-formation onward are quite accurate, with track forecast spreads that are primarily related to initial position uncertainties. The ECEPS intensity forecasts have been validated relative to the Joint Typhoon Warning Center (JTWC) Working Best Track (WBT) intensities (when available). The key results for Tokage (11 W) were the ECEPS forecasts of the intensification to a peak intensity of 100 kt, and then a rapid decay as a cold-core cyclone. For Hinnamnor (12 W), the key result was the ECEPS intensity forecasts during the post-extratropical transition period when Hinnamnor was rapidly translating poleward through the Japan Sea. For Muifa (14 W), the key advantage of the ECEPS was that intensity guidance was provided for longer periods than the JTWC 5-day forecast. The most intriguing aspect of the ECEPS forecasts for post-Merbok (15 W) was its prediction of a transition to an intense, warm-core vortex after Merbok had moved beyond 50° N and was headed toward the Aleutian Islands. The most disappointing result was that the ECEPS over-predicted the slow intensification rate of Nanmadol (16 W) until the time-to-typhoon (T2TY), but then failed to predict the large rapid intensification (RI) following the T2TY. The tentative conclusion is that the ECEPS model's physics are not capable of predicting the inner-core spin-up rates when a small inner-core vortex is undergoing large RI.

Keywords: tropical cyclone track forecasts; ensemble model predictions; Rossby wave breaking events



Citation: Elsberry, R.L.; Tsai, H.-C.; Chin, W.-C.; Marchok, T.P. ECMWF Ensemble Forecasts of Six Tropical Cyclones That Formed during a Long-Lasting Rossby Wave Breaking Event in the Western North Pacific. *Atmosphere* **2024**, *15*, 610. <https://doi.org/10.3390/atmos15050610>

Academic Editors:

Ching-Yuang Huang, Shu-Ya Chen, Kao-Shen Chung and Jimmy Dudhia

Received: 29 March 2024

Revised: 21 April 2024

Accepted: 26 April 2024

Published: 17 May 2024



Copyright: © 2024 by the authors. Licensee MDPI, Basel, Switzerland. This article is an open access article distributed under the terms and conditions of the Creative Commons Attribution (CC BY) license (<https://creativecommons.org/licenses/by/4.0/>).

1. Introduction

1.1. Motivation

There are several review articles from the 10th International Workshop on Tropical Cyclones that provide the context for this submission to the *Special Issue on Typhoon/Hurricane Dynamics and Prediction*. Operational warning agencies have achieved major improvements in tropical cyclone (TC) track forecasts by utilizing a consensus of numerical model track forecasts, but the rate of improvement has been slowing in recent years (Conroy et al., 2023) [1]. Most TC warning centers utilize an unweighted consensus (i.e., assume all model tracks are equally likely) that usually is a combination of deterministic models, although a

growing number of centers also include unweighted ensemble mean track forecasts (again, assuming all ensemble member track forecasts are equally likely). Conroy et al. [1] describe an example of the Joint Typhoon Warning Center (JTWC) unweighted consensus tracker (CONW; Sampson and Schrader, 2000 [2]) that consists of nine members (six deterministic models and three ensemble models). The consensus tracker shifts each model track forecast in space and time to match the recent working best-track position analyzed by the JTWC. The forecaster does have the option to select/omit among the CONW member track forecasts based on known model biases and the previous forecast. Conroy et al. ([1], their Figure 1) present as an example of a difficult CONW forecast the track of Tropical Storm 16 W initialized at 1200 UTC 14 September 2022, which started at $\sim 23^\circ$ N, 140° E after an anticyclonic loop, and later translated northwestward to make landfall on southern Japan. Coincidentally, TS 16 W was one of a sequence of six TCs during August–September 2022 that had difficult track forecasts, which we attribute to these six TCs forming at higher latitudes (20 – 25° N) in association with a long-lasting Rossby wave breaking (RWB) event.

Conroy et al. [1] note an increased use of ensemble mean tracks to improve track forecast guidance, and to issue situation-dependent depictions of track uncertainty. In this study, we utilize the European Centre for Medium-Range Weather Forecasts' ensemble prediction system (ECEPS) to demonstrate its capability to predict those six TCs. Since these are 15-day forecasts, the review by Schreck et al. (2023) [3] of advances in TC prediction on subseasonal time scales is also background for this study. Indeed, Schreck et al. ([3]; their Figure 8) provide an example from the Elsberry et al. (2022) [4] ECEPS track, formation, and ending forecasts of the lifecycle of Hurricane Linda (2021) in the eastern North Pacific. In contrast to the unweighted ensemble models mentioned above, our weighted mean vector motion (WMVM) track forecast gives the greatest (smallest) weight to the ensemble member tracks that have 12 h vector motions that most (least) closely resemble the previous 12 h WMVM vector, and thus tend to "go down the middle" of the cluster of member tracks. Finally, the recent review by Wadler et al. (2023) [5] of research on the external influences on TC intensity change is relevant to our ECEPS-based intensity predictions of these six RWB-related TCs.

While not a review article, Wang et al. (2023) [6] describe another of the six TCs (Super Typhoon Hinnamnor) that formed in association with that summer 2022 long-lasting RWB event and exhibited all of the major features that pose current challenges in typhoon research. During the lifecycle of Hinnamnor, it (1) experienced a sudden change of track; (2) underwent a two-phase RI with an intermediate eyewall replacement cycle; (3) interacted with another vortex that later merged into the Hinnamnor outer circulation; (4) expanded in size; (5) produced a strong cold wake; (6) underwent rapid weakening; and (7) underwent an extratropical transition. Wang et al. [6] describe all of these challenges, and propose that research studies of cases such as Hinnamnor could advance our understanding of the dynamics and physical processes of TCs. Furthermore, Wang et al. [6] propose that Hinnamnor could serve as a benchmark for validating different numerical model predictions of typhoon tracks, intensities, and structural changes. Thus, this study of the six TCs that formed during a long-lasting RWB event during August–September 2022 is contributed to this Special Issue.

1.2. Background on RWB Events and TCs in Western North Pacific

As described by Enomoto et al. (2003) [7], Rossby wave propagation along the Asian jet in association with the summer-time southwest monsoon over east Asia frequently leads to an RWB event near the jet exit over the western North Pacific (WPAC) southeast of Japan. Takemura et al. (2017) [8] studied an RWB event during August 2016 in which a high potential vorticity (PV) intrusion moved equatorward to create enhanced deep convection over the subtropical WPAC. Enhancement of the WPAC monsoon trough led to six TC formations during the month of August. Takemura and Mukougawa (2021) [9] then summarized WPAC TC formations and the subsequent tracks that occurred in association with RWB events (Figure 1). Note that during the peak summer monsoon, there is a large

north–south PV gradient over east Asia, but a much weaker-gradient PV off the east Asia coast that leads to the RWB event. A large PV intrusion (Figure 1c, yellow region) extends southwestward toward the tropics (reference point in each panel is at 32.4° N, 160.9° E). The few pre-TC circulations that develop at Day 4 (Figure 1d) tend to drift westward rather than recurve. As the RWB anticyclonic circulation amplifies and the PV intrusion extends westward at Day 2 (Figure 1e), many more TCs develop and many of those TCs have recurving tracks (Figure 1f). At Day 0 (Figure 1g), the PV intrusion has closed off and the number of TC developments in relation to the RWB event increases. Nearly all of those TCs have recurving tracks (Figure 1h) around the western boundary of the closed-off PV intrusion (Figure 1g).

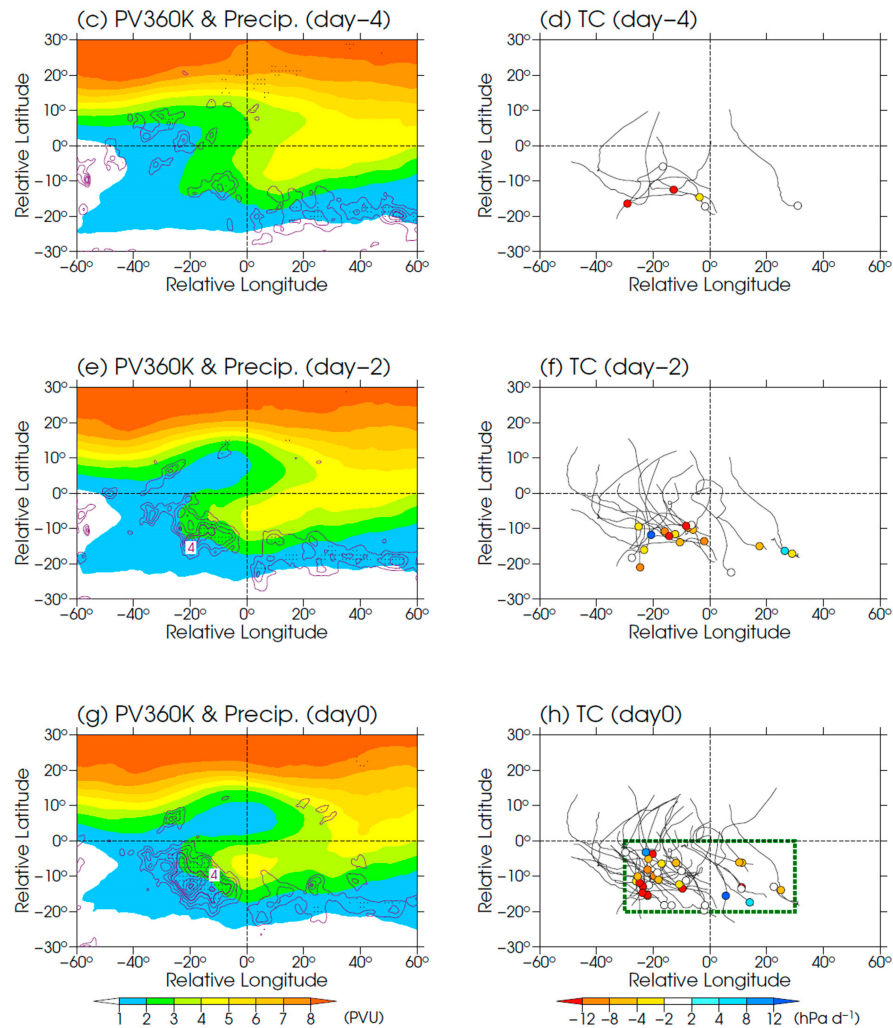


Figure 1. Modified composites by Takemura and Mukougawa [9] of (left) 300 K potential vorticity (PV) and (right) relative positions of TC developments (circles) and subsequent tracks (gray lines) relative to the coordinate origin that corresponds to the Rossby wave breaking (RWB) center at 32.4° N, 160.9° E. (c,d) Day 4, (e,f) Day 2, and (g,h) Day 0 relative to the peak frequency of TC developments. See (a) and (b) in Takemura and Mukougawa [9] for additional details.

Takemura and Mukougawa [9] present composites relative to the RWB reference point of atmospheric features and the sea-surface temperature (SST) that are favorable for TC formation. Strong 925 mb convergence, and enhanced convection, is documented well to the southwest of the RWB event center where low-level easterlies interact with the monsoon southwesterlies. Although warm SST anomalies exist in the southwest quadrant of the RWB event, the vertical wind shear is also enhanced over the southwest quadrant in association with the PV intrusion aloft (Figure 1). Thus, Takemura and Mukougawa [9]

suggest that it is the RWB-related enhanced convection that has the essential role in the TC formation locations in Figure 1d,f, and 1h. Fudeyasu and Yoshida (2019) [10] suggest that the subsequent poleward motion of the TCs is associated with the upper-tropospheric southerly winds over the southwest quadrant. The recurvature longitude tends to be ~25 degrees to the west of the RWB reference point ([10], their Figure 5b).

The Schreck et al. [3] review includes a number of studies on similar Atlantic TC formations in relation to PV streamers (i.e., between the RWB anticyclone to the north and the PV intrusion to the south) in association with RWB events. For example, Galarneau et al. (2015) [11] studied 12 TCs during 2004–2008 that developed within one Rossby radius of PV streamers associated with the mid-Atlantic trough identified previously as the tropical upper-tropospheric trough. Papin et al. (2020) [12] identified 21,149 PV streamers in the North Atlantic during June–November 1979–2015 with a peak in July–August. However, their focus was on seasonal TC activity rather than relating their new PV streamer index to specific TC events as in this study. On the other hand, Zhang et al. (2017) [13] separately studied RWB events in the western Atlantic versus in the eastern Atlantic, and concluded that RWB occurrences in the western basin were more likely to hinder TC intensification or reduce the TC lifetime. Similarly, Li et al. (2018) [14] studied the subseasonal variability of RWB and found it suppressed Atlantic TC activity on the subseasonal timescale.

1.3. Six TCs Related to August–September 2022 RWB Events

Although we did not calculate composites of the 300 K PV fields as in Figure 1 by Takemura and Mukougawa [9], the formation locations and tracks of the six TCs in Figure 2 are consistent with them having an origin in relation to an RWB event. Note in Figure 2 that Typhoon Tokage (11 W) and Super Typhoon (STY) Hinnamnor (12 W) originate at almost the identical location near 22° N, 151° E. Tokage almost immediately becomes a TS at 0600 UTC 22 August and then a TY at 0600 UTC 23 August (Table 1, row 1). Tokage continues as a TY until 0000 UTC 25 August as it moves poleward and recurves. The last JTWC Working Best Track (WBT) has Tokage as a TS (35 kt) as it approaches 50° N (Figure 2).

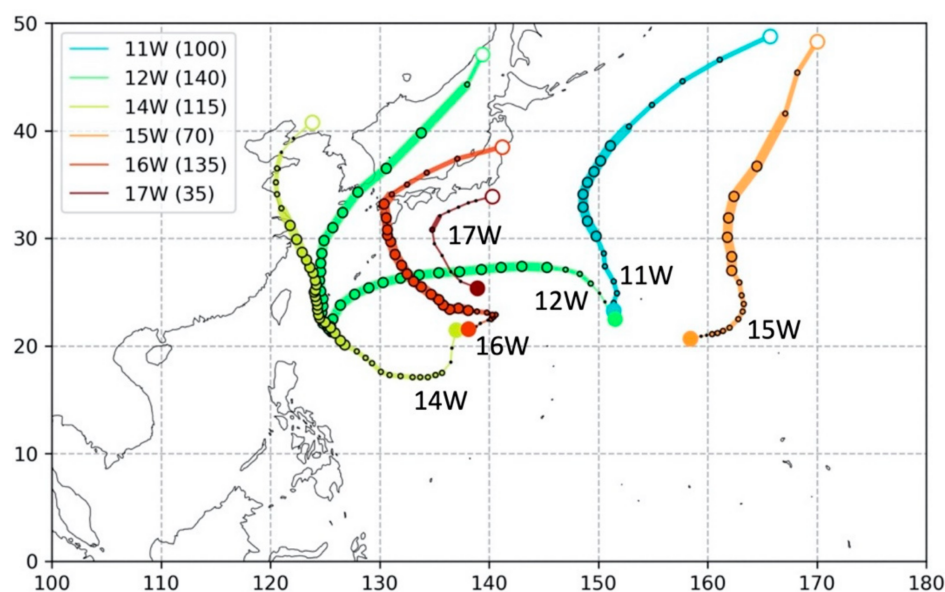


Figure 2. Six TC tracks (color definitions, JTWC numbers, and peak intensities [kt] in inset in upper left) during August–September 2022. Along each track, thin line connecting black dots at six-hour intervals denotes pre-TS intensities, medium line thickness connecting small circles denotes period of TS intensities, and wider line thickness connecting larger circles denotes TY intensities.

Table 1. Key times (MMDDHH) from the Working Best Track (WBT) files for the six TCs, including times of first WBT value, tropical storm (TS), typhoon (TY), ending TY, and last WBT value.

	First WBT	TS	TY	Ending TY	Last WBT
Tokage (11 W)	082100	082206	082306	082500	082606
Hinnamnor (12 W)	082700	082806	082900	090606	090618
Muifa (14 W)	090412	090700	090918	091418	091612
Merbok (15 W)	091006	091112	091318	091500	091518
Nanmadol (16 W)	091100	091318	091506	091818	092000
Talas (17 W)	092000	092300	--	--	092412

Recall that Wang et al. [6] presented STY Hinnamnor (12 W) as an example of the current challenges in typhoon research and forecasting. Hinnamnor had an extremely challenging track to forecast (Figure 2). Even though Hinnamnor (12 W) started only 6 days after Tokage (11 W) (Table 1), Hinnamnor moved poleward, but quickly turned westward rather than recurving. Hinnamnor had rapidly intensified from a TS at 0600 UTC 28 August to a TY in only 18 h (Table 1, row 2). The second large track forecast challenge was when Hinnamnor (12 W) turned southward after crossing 130° E and became quasi-stationary near 22° N, 125° E. In conjunction with an eyewall replacement cycle [6], Hinnamnor decreased in intensity from a peak value of 140 kt at 0000 UTC 1 September to 75 kt at 1200 UTC 2 September before re-intensifying to 110 kt at 0600 UTC 4 September (JTWC WBT). As indicated in Figure 2, Hinnamnor continued moving poleward at TY intensity until reaching 40° N at 0600 UTC 6 September (Table 1, row 2). Hinnamnor continued only another 12 h before making landfall (Figure 2).

Strong TY Muifa (14 W) had another difficult track to forecast (Figure 2). After starting at 12 UTC 4 September near 22° N, 137° E, Muifa moved to the south before becoming a TS at 0000 UTC 7 September (Table 1, row 3). Even though Muifa was over 30 °C water ([6], their Figure 1), the intensity remained near 40 kt until 0000 UTC 9 September (JTWC WBT). Within 18 h, Muifa was a TY, and a peak intensity of 115 kt was achieved at 0000 UTC 11 September (JTWC WBT). As indicated in Figure 2, the Muifa track was overlying the path of STY Hinnamnor when Hinnamnor was quasi-stationary on 2 September (about 8 days earlier). Nevertheless, Muifa maintained an intensity of ~85 kt from 0000 UTC 12 September to 0600 UTC 14 September (JTWC WBT) as Muifa approached the east coast of China. The intensity decay was rapid as landfall was made (Figure 2).

At the same time Muifa (14 W) was becoming a TY east of Taiwan, Merbok (15 W) was quickly becoming a TS (Table 1, row 4) far to the east near 21° N, 160° E (Figure 2). The track and intensity evolutions of Merbok were similar to those of Tokage (11 W). That is, the tracks were poleward, and although Merbok only reached a maximum wind speed of 70 kt at 0600 UTC 14 September, TY intensity continued until 40° N, and TS intensity continued until Merbok was also approaching 50° N, near 170° E (Figure 2). The large translation speeds for both Merbok (15 W) and Tokage (11 W) north of 40° N would be very difficult to forecast.

Almost at the same time as Merbok (15 W) was developing to the east, Super Typhoon Nanmadol (16 W) was developing at almost the same location (22° N, 138° E) where TY Muifa (14 W) had developed 7 days earlier (Table 1, rows 5 and 3, respectively). Nanmadol initially drifted toward the northeast and became stationary near 23° N, 140° E (Figure 2). However, Nanmadol then began a classical recurvature track, and TY intensity was achieved at 0600 UTC 15 September (Table 1, row 5), which made it the fifth TY in

23 days. Rapid intensification to 135 kt occurred at 1800 UTC 16 September (JTWC WBT). However, slow decay began until landfall occurred on southern Japan (Figure 2). Nanmadol continued as a TS to move rapidly to the northeast over the Japan Sea until a second landfall on Hokkaido.

Finally, weak TS Talas (17 W), which according to the JTWC had a peak intensity of 35 kt for only a short time (0000 UTC 23 September; Table 1, row 6), was included for several reasons. First, Talas (17 W) started quite close to where Muifa (14 W) and Nanmadol (16 W) started (Figure 2). Second, the recurvature track of Talas was quite similar to that of Nanmadol (16 W). Third, the Talas recurvature track came quite close to the southern coast of the Japanese mainland and could have had a large impact if a TY had developed.

In summary, Wang et al. [6] proposed STY Hinnamnor (12 W) as an example of the current challenges in typhoon research and forecasting, and Conroy et al. [1] presented Nanmadol (16 W) as a challenging track forecast. As indicated in Figure 2, all five TYs (11 W–16 W) that developed in association with the long-lasting Rossby wave breaking event had challenging track forecasts. It is definitely a challenge to forecast the formation locations and early track segments for TCs that develop between 20° N and 25° N. In addition, all six TCs had recurvature-type track forecasts, and three (11 W, 12 W, and 15 W) had long post-recurvature tracks moving rapidly, which are a challenge to forecast. Hinnamnor (12 W) and Muifa (14 W) existed for 10 days and 12 days, respectively, and had the most difficult track and intensity forecasts.

Wang et al. [6] mention that Hinnamnor (12 W) produced a strong cold ocean wake, which is consistent with its TY intensities along the westward path and along the long poleward track to 45° N (Figure 2). Then, Muifa (14 W) moved along that poleward cold wake of Hinnamnor over much of its lifecycle. Nanmadol (16 W) later crossed over the westward cold wake of Hinnamnor, as did TS Talas (17 W). Such cold wake interactions make intensity forecasting more challenging [5].

1.4. Objectives

Each of these six TCs present forecast challenges, beginning with the formations between 20° N and 25° N in conjunction with a long-lasting RWB event. As illustrated in Figure 2, even though the formation locations may be close in space and time, the subsequent tracks may be quite diverse. The objective of this study is to demonstrate the capability of the ECEPS to forecast the formation, track, and intensity of these six TCs. It is noted that our weighted mean intensity of the ECEPS member intensities is also provided from Marchok (2021) vortex tracker files [15]. This weighted mean intensity is most effective for the tropical depression stage. However, it will also be documented that it is quite effective during the late decay stage, and the following extratropical transition.

A brief description of our version of the ECEPS will be given in Section 2. An overview of the ECEPS WMVM track forecasts for the six TCs will be presented in Section 3 along with a summary of the intensity forecasts of RI events following formation. For the five TYs, a focus will be on the capability of the ECEPS forecasts of the intensity decay, because a majority of the TYs decay either in coastal regions, or in the main shipping route between Asia and the United States.

2. Development of ECEPS-Based Formation, Tracks, and Intensity Forecasts

Over the past five years, our research team has investigated the capability of the ECEPS to predict WPAC TC formation, track, and intensity. For example, Tsai et al. (2020) [16] demonstrated an opportunity to provide early (10 days in advance) warnings of the formation, intensification, and subsequent track of Typhoon Lekima (2019). In addition to the time-to-formation (either 25 kt or 35 kt) timing and positions along the WMVM track forecasts, seven-day intensity forecasts after the formation were provided using a weighted analog intensity technique. Although not an RWB event, Lekima did form somewhat farther north (~18° N), had a northwestward track similar to the tracks in Figure 2, and made landfall on the East China coast south of Shanghai six days after formation. Thus, the

availability of these ECEPS forecasts would have provided early guidance as to the heavy rains and floods that accompanied the Lekima landfall.

In an advanced version of the ECEPS applied in the eastern North Pacific and the Atlantic as well, Elsberry et al. (2020) [17] further demonstrated the application of the ECEPS's weighted analog intensity technique. The objective was to demonstrate the earlier (up to 5 days) formation timing and position guidance, and to provide the intensity guidance for longer (up to 15 days) along the WMVM track forecast. For example, the forecast of pre-Hurricane Kiko in the eastern North Pacific indicated that Hawaii would be under threat by the end of the 15-day ECEPS WMVM track forecast.

Elsberry et al. (2021) [18] demonstrated the capability of the ECEPS to predict rapid intensification (RI: 30 kt/24 h) events for a sequence of WPAC TCs during 2019. The ECEPS predictions of the warm-core magnitudes (WCMs) of pre-TC circulations were utilized to define time-to-formation (defined as 35 kt), and to estimate the likely storm category. The ECEPS predictions of the WCMs of pre-TC circulations were utilized to calculate the time-to-formation (defined as 35 kt). If that category was a typhoon, a bifurcation version of the Tsai et al. [15] intensity technique better predicted the RI events by selecting only Cluster 1 analog storms with the largest peak intensities. Validations were in terms of (i) detection time in advance of formation; (ii) accuracy of time-to-formation; (iii) intensification stage prediction; and (iv) peak intensity magnitude/timing. This modified technique was demonstrated to provide earlier guidance as to the threat of an RI event following formation that would lead to a typhoon along the 15-day ECEPS track forecast.

A substantial advancement was made when the previous studies of WPAC track, formation, and intensity predictions along the 15-day ECEPS track forecasts were extended to the eastern North Pacific (ENP) during the 2021 hurricane season (Elsberry et al. (2022) [4]. First, earlier forecasts were provided of the Time-to-TS (T2TS) and the Time-to-Hurricane (T2HU) and Time-to-Ending Tropical Storm (TETS) times and positions along the WMVM track forecasts. Elsberry et al. [4] utilized the same track weighting factors to give the largest weight in the weighted mean warm-core magnitude (WCM) calculation along the WMVM forecast. After some testing, the appropriate ECEPS-predicted WCM threshold values for the ENP storm intensities were maximum WCM < 25.0 for a tropical depression; $25.0 < \text{WCM} < 37.0$ for a tropical storm; and $\text{WCM} > 37.0$ for a hurricane. The capability of the ECEPS to forecast not only the T2TS and T2HU timings and positions during the intensification stage, but also the TEHU and the TETS timing and positions during the decay stage for ENP Hurricane Linda (2021), was recognized in the Schreck et al. [3] review. Elsberry et al. (2023) [19] provided a decision flowchart to assist the forecasters to select the pre-formation disturbance that is most likely to become the next TS with a potential to become a hurricane in the ENP.

For the 2022 season, the focus switched back to the WPAC, and an ECEPS-based lifecycle prediction version was developed and tested from 5 August 2022 to 20 January 2023. Daily, or sometimes twice daily, forecasts were provided to the Joint Typhoon Warning Center (JTWC). No changes were necessary for the ECEPS WMVM track forecasts. After some testing, the weighted mean WCM threshold for a typhoon was changed from 37.0 in the ENP to 47.0. Analyses and validation of the final version of the western North Pacific forecasts for 11 W through 26 W have been continuing after some delays.

As was the case for Elsberry et al. [4,20] in the ENP, we confirmed that the adjusted WCM-based intensities could be utilized to estimate the T2TS, T2TY, TETY, and TETS timing and location along the WMVM track forecasts. Therefore, we then developed the code utilizing the weighted mean WCM relationship with intensity that has linear segments connecting the tropical depression, TS, TY, and the allowable peak intensity threshold values to predict the ensemble storm weighted mean intensity in the WPAC throughout the entire lifecycle beginning from the pre-formation stage. We noted that the JTWC sometimes provides intensity guidance beyond 35° N for post-recurvature TCs. The ECEPS-predicted evolution along those WMVM track forecasts can provide the extratropical transition (WCM = 0) timing and location, and

then the direct ECEPS weighted mean intensity provides guidance for the intensity during the cold-core stage.

Early in the study period, we noticed that many of the storm options during Week 1 continued to exist for 14 days. While our prior focus had been on 6-hourly positions and intensities for 7 days to just predict the T2TS and T2TY, we changed to 12-hourly positions and intensities for 14 days to predict the lifecycle threat of WPAC TC high winds and seas. Our guiding principle has always been that the TC intensity beyond 72 h is primarily determined by the track forecast. Thus, these WPAC lifecycle intensity forecasts will only be as good as the ECEPS WMVM track forecasts. This study has demonstrated, first in the ENP, and now in the WPAC, that the ECEPS WMVM track forecasts are highly skillful, from the pre-formation stage to the extratropical transition stage. Consequently, our objective was expanded to document the ECEPS's capability to provide (i) earlier pre-formation guidance of the formation, track, and intensity of WPAC TCs; and (ii) longer track and intensity forecasts of up to 14 days of the lifecycle of those TCs, which may include the extratropical transition stage.

3. ECEPS Forecasts of Rossby Wave Breaking Event with a Sequence of Six WPAC Storms

The western North Pacific TC occurrences in the six weeks before our WPAC study that started on 5 August 2022 were unusual. TY Chaba (04 W), with a peak intensity of 75 kt, and TS Aere (05 W), with a peak intensity of 45 kt on 2 July, co-existed between 29 June and 11 July. However, then, no TC activity occurred until TD Songda (06 W) and TD Trases (07 W), both with $V_{max} = 30$ kt, which co-existed between 29 July and 2 August, and TD Eight, which existed for one day (4 August). Early in our study, TS Meari (09 W) started on 11 August at a high latitude (28.8° N, 135° E) and reached a peak intensity of only 40 kt on 14 August near 43.6° N, 149.2° E. Although TS Meari may have been related to the long-lasting RWB event, the connection is not so clear, and the intensity was only that of a TS. Finally, TS Ma-on (10 W) began on 21 August east of the Philippines near 17.0° N, 126.3° E and moved west-northwest to reach a peak intensity of 55 kt near 21.0° N, 102.7° E. As presented in Figure 2, 11 W–16 W and TS Talas (17 W) then developed within 20° N– 25° N and 140° E– 160° E.

An overview of the ECEPS track forecasts for the six TCs is provided in Figure 3, with the color codes for the individual ECEPS forecasts in the insets. For example, in Figure 3a for TY Tokage (11 W), there are 14 forecasts, and, except for the starting track segments, the track spread is quite small. For long-lasting TY Hinnamnor (12 W) in Figure 3b, there are 24 forecasts. Unfortunately, for the duration of the period with the unusual westward path, there are many missing ECEPS forecasts. Although co-author Timothy Marchok was able to re-run selected forecasts as cold starts, the accuracy was not comparable with the continuous warm-start track forecasts. One of the special features of TY Hinnamnor noted by Wang et al. [6] was the interaction with another vortex that later merged into the Hinnamnor outer circulation. At least one ECEPS forecast (orange) started near 20° N, 140° E and moved westward to merge with the main vortex (Figure 3b).

The 32 ECEPS forecasts for TY Muifa (14 W) in Figure 3c had the largest track spread. During the early southward and then westward track segment, when the pre-formation Muifa vortex was moving over high ocean temperatures ([6], their Figure 1), the ECEPS repeatedly would over-develop the vortex. However, formation, defined as 35 kt, did not occur until 0000 UTC 7 September (Table 1, row 3). By contrast, the first JTWC WBT time was not until 1200 UTC 4 September (Table 1, row 3), which was the time of the ninth ECEPS forecast, shown in Figure 3c. TY Merbok (15 W) also was the subject of many (22) ECEPS forecasts (Figure 3d). The larger track forecast spread was clearly due to the large uncertainty in the starting positions. The first JTWC WBT time was not until 0600 UTC 10 September (Table 1, row 4), which was the time of the 12th ECEPS forecast in Figure 3d. Thus, the ECEPS forecasts were giving early guidance as to the next TY, but there was considerable uncertainty about the starting position. Similar comments apply to TY Nanmadol, because the first JTWC WBT at 0000 UTC 11 September (Table 1, row 5)

was at the time of the ninth ECEPS forecast, shown in Figure 3c. While there is a large scatter in those first nine track forecasts, once Nanmadol became a TS at 0600 UTC 15 September, these ECEPS recurvature-type forecasts had a relatively small spread. Finally, it is not surprising that pre-TS Talas (17 W), which had a peak intensity of 35 kt, had a large ECEPS track forecast uncertainty in the initial positions (Figure 3f). The European Centre for Medium-Range Weather Forecasts (ECMWF) does not bogus the position or intensity of tropical storms or typhoons, let alone a pre-TS circulation.

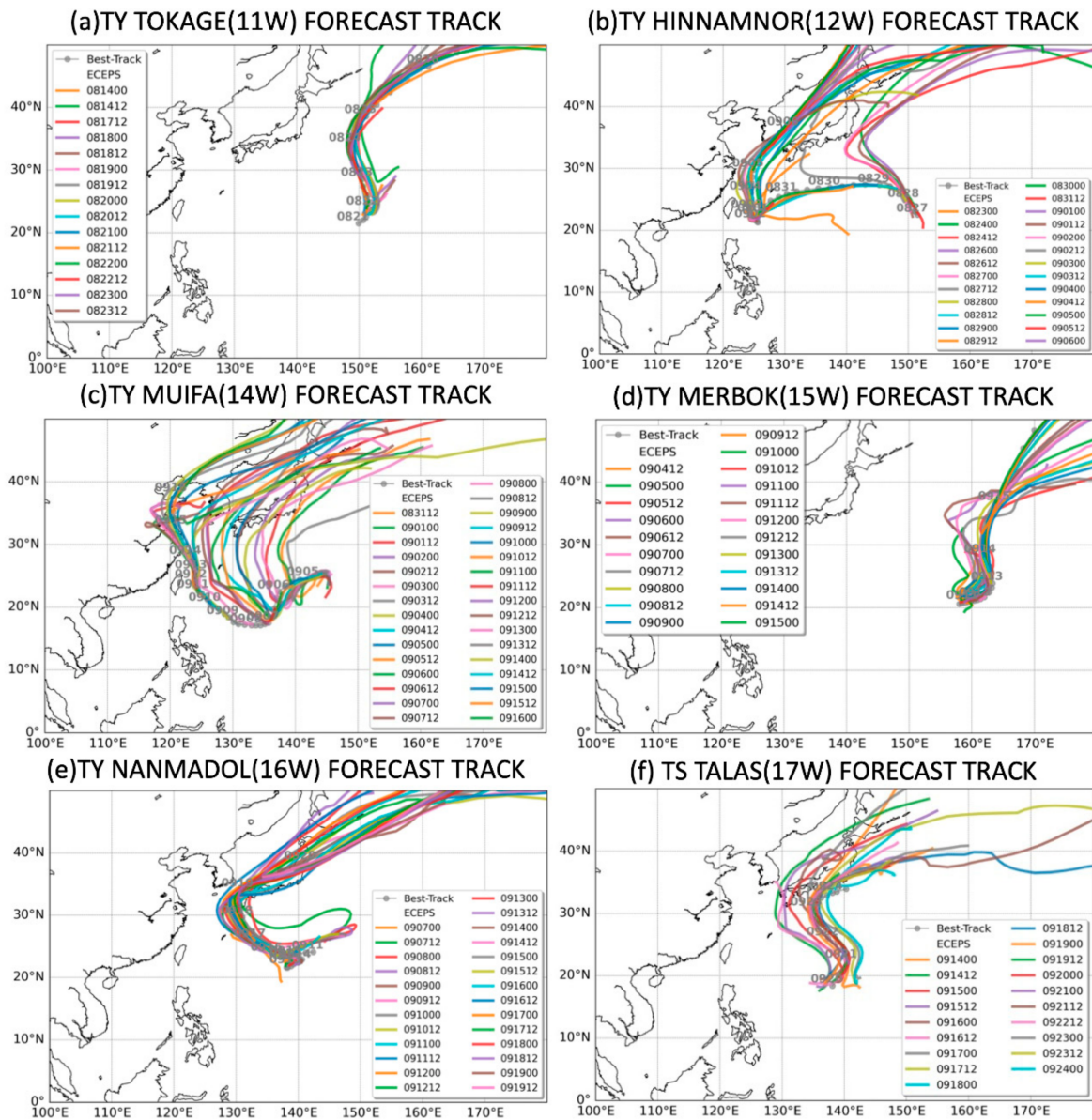


Figure 3. Weighted mean vector motion (WMVM) track forecasts (track colors defined in inserts) of the ECEPS and JTWC best tracks (black dots with labels at 0000 UTC) for (a) TY Tokage (11 W), (b) TY Hinnamnor (12 W), (c) TY Muifa (14 W), (d) TY Merbok (15 W), (e) TY Nanmadol (16 W), and (f) TS Talas (17 W).

The two tables below document early detections for both the time-to-tropical storm (T2TS) and time-to-typhoon (T2TY) for TYs 12 W through 26 W [20]. As was the case for Elsberry et al. [4,20] in the ENP during the 2021 hurricane season, we confirmed that the adjusted warm-core magnitude-based forecast intensities could be utilized in the WPAC to also estimate T2TS and the T2TY timings and locations along the WMVM track. In

the WPAC, we only searched back 7 days prior to the T2TS for the first detection of the disturbance that had a track matching the track of the target typhoon (Table 2 (a)). Note that in column 3, all of these nine typhoons except Hinnamnor (12 W) had early detections as likely TSs at around the maximum search time of 7 days. Furthermore, the T2TY early detection times for those disturbances that became one of these TYs were as short as 6 days, for TY Hinnamnor (12 W), to 10 days 18 h, for TY Nalgae (26 W). Thus, our technique could greatly improve decision making related to the timing and the location of high winds associated with WPAC typhoons.

Table 2. (a) ECEPS early detections within 7 days before T2TS and early detections before T2TY for western North Pacific typhoons during the last half of the 2022 season. [20]. (b). JTWC Working Best Track indication of an RI occurrence (column 2) or non-occurrence (column 4), and ECEPS correct prediction of RI event occurrence (column 3) or RI non-occurrence (column 5) at early prediction time of an RI event (T2TY–T2TS) < 24 h following T2TS.

(a)				
Typhoon	T2TS	Early Detection	T2TY	Early Detection
Tokage (11 W)	0000 UTC 22 August	8 days, 0 h	0600 UTC 23 August	9 days, 0 h
Hinnamnor (12 W)	0006 UTC 28 August	5 days, 6 h	0800 UTC 29 August	6 days, 0 h
Muifa (14 W)	0000 UTC 7 September	7 days, 12 h	1800 UTC 8 September	10 days, 6 h
Merbok (15 W)	1200 UTC 11 September	7 days, 0 h	1800 UTC 13 September	9 days, 6 h
Nanmadol (16 W)	1800 UTC 13 September	6 days, 18 h	0600 UTC 15 September	8 days, 6 h
Noru (18 W)	0600 UTC 22 September	6 days, 18 h	0600 UTC 24 September	8 days, 18 h
Kulap (19 W)	0000 UTC 26 September	7 days, 0 h	1200 UTC 28 September	9 days, 12 h
Roke (20 W)	1200 UTC 28 September	7 days, 0 h	0600 UTC 29 September	7 days, 18 h
Nesat (23 W)	0600 UTC 15 October	6 days, 18 h	0600 UTC 16 October	7 days, 18 h
Nalgae (26 W)	1200 UTC 27 October	7 days, 0 h	0600 UTC 31 October	10 days, 18 h

(b)				
Typhoon	RI Occurrence Following T2TS	Correct Prediction of Occurrence	Non-Occurrence of RI Event	Correct Prediction of Non-Occurrence
Tokage (11 W)	Maybe (30 h)	Yes (24 h)		
Hinnamnor (12 W)	Maybe (26 h)	Yes (18 h)		
Muifa (14 W)			Yes (42 h)	Yes (66 h)
Merbok (15 W)			Yes (54 h)	Yes (34 h)
Nanmadol (16 W)	Maybe (36 h)	Maybe (36 h)		
Noru (18 W)			Yes (48 h)	Yes (48 h)
Kulap (19 W)			Yes 60 h)	Yes (60 h)
Roke (20 W)	Yes (18 h)	Yes (18 h)		
Nesat (23 W)	Yes (24 h)	Yes (24 h)		
Nalgae (26 W)			Yes (90 h)	Yes (90 h)

A high-priority research objective during the last decade has been to improve predictions of rapid intensification (RI), which in this study is defined as an increase of 30 kt within 24 h. The existence of such an RI event following the T2TS time is particularly important because that means typhoon-force (64 kt) winds could threaten maritime activities within a day of TC formation time. In Table 2 (b), the occurrence of an RI event following formation is defined from Table 2 (a) as (T2TY–T2TS) < 24 h (i.e., time in column 4 minus time in column 2 is less than or equal to 24 h). Whether that RI occurrence following T2TS is correctly predicted by the ECEPS is assessed by the TY detection time in column 5 minus the TS detection time in column 3 being less than or equal to 24 h. Including the close (26 h) RI event following the formation of TY Hinnamnor (12 W), there were only three RI occurrences following its formation among these nine TYs. It is noteworthy that, as shown in Table 2 (b), all four RI occurrences were correctly predicted with early (7 days) detections of the disturbance in the ECEPS forecasts. It is also important that these ECEPS

forecasts provided accurate guidance as to the non-occurrence of RI following formation for the other six TYs since that provides extra time until TY-stage winds will occur along the WMVM track forecast.

4. Validations of ECEPS Forecasts for the Six Tropical Cyclones

Validation of the ECEPS intensity forecasts for the six TCs will be relative to the JTWC WBT when available. Due to the almost 12 h delay before the ECEPS files are available at the JTWC from the Marchok [15] website, the ECEPS T + 12 h forecast and beyond will also be compared with the corresponding JTWC forecast beginning at the T + 12 h time. Recall that the ECEPS initialization does not include any intensity information from the TC Vitals. As is common with model validations, ECEPS intensity forecasts will be adjusted to begin with the JTWC intensity at T + 12 h. The objective is not to calculate statistical differences because the JTWC (ECEPS) intensities are digitized to the nearest 5 kt (1 kt). Rather, the purpose is to demonstrate that our ECEPS intensity forecast technique could provide earlier (pre-formation) and/or extended (only 7-day forecasts are shown here, but 14-day forecasts are created) guidance.

4.1. Challenges and Opportunities for TY Tokage (11 W)

Whereas the first entry in the JTWC Working Best Track (WBT) for Tokage was at 0000 UTC 22 August, the first detection of the disturbance in the ECEPS was at 0000 UTC 14 August (early detection by 8 days; Table 2 (a), row 1). Unfortunately, there was a gap in the ECEPS forecasts until 1200 UTC 17 August, but then the ECEPS forecasts were continuously available and provided highly accurate (+/− 24 h) time-to-tropical depression, time-to-TS, and time-to-TY predictions. A special circumstance in the intensity validation table for Tokage (Figure 4) is that the JTWC WBT intensity values did not begin until 45 kt at 1200 UTC 22 August—presumably because the forecasters considered Tokage to be a cold-core system prior to that time.

The warm-core magnitude (WCM) predicted by the ECEPS is positive (negative) for a warm-core (cold-core) TC (subtropical cyclone). The pre-Tokage disturbance in the 0000 UTC 21 August ECEPS initial conditions had a cold-core disturbance with weak boundary layer (540 m) winds of 23 kt. However, that disturbance was predicted to become (warm-core) TS Tokage with an intensity of 39 kt at 12 UTC 22 August, and a peak intensity of 71 kt at 0000 UTC 24 August (Figure 4, row 1). The ECEPS then predicted Tokage would again become cold-core in 24 h with an intensity of 30 kt, and continue at that intensity for another three days as Tokage rapidly moved poleward to the east of Japan (Figure 2). From the time of the first JTWC forecast at 12 UTC August, the ECEPS forecasts of the Tokage intensification to the peak intensity of 100 kt at 0000 UTC 24 August, and then a rapid decay as a cold-core cyclone, were generally quite good. After that first JTWC (under) forecast, their forecasts of the intensification to peak intensity and the beginning of the decay were also good, but JTWC tended to drop the later stages of Tokage as an indication of extratropical transition. In summary, the ECEPS WCM predictions would assist the JTWC in analyzing (including interpretation of satellite imagery) and forecasting the intensity of subtropical cyclone disturbances, their transition to TCs, and then the extratropical transition of TCs such as TY Tokage.

ECEPS Date/Time	22/00		23/00		24/00		25/00		26/00		27/00		28/00	
	22/12		23/12		24/12		25/12		26/12		27/12		28/12	
	[35]	[45]	[60]	[80]	[100]	[85]	[70]	[45]	[40]	[45]	[40]			
21/00Z (21/12Z)	23	39	52	63	71	54	30	32	33	30	26	23	27	
21/12Z (22/00Z)	31	52	58	73	81	49	29	29	31	27	23	18	16	27
22/00Z (22/12Z)	29	59 (45)	67 (50)	78 (65)	81 (60)	54 (60)	32 (55)	33 (50)	34 (43)	28 (35)	27	28	26	25
22/12Z (23/00Z)			80 (60)	90 (70)	94 (80)	77 (85)	47 (70)	32 (55)	31 (40)	28	25	22	23	27
23/00Z (23/12Z)			93 (80)	98 (100)	102 (130)	86 (75)	50 (60)	39 (50)	33 (40)	27	23	23	26	
23/12Z (24/00Z)					97 (100)	101 (90)	87 (80)	53 (70)	38 (55)	34	26	18	22	
24/00Z (24/12Z)					80 (85)		55 (70)	40 (60)	37 (50)	27	19	18	19	
24/12Z (25/00Z)							63 (70)	41 (50)	37 (40)	29	21	16		

Figure 4. Validation of ECEPS and (JTWC) intensity forecasts (kt) for Tokage (11 W) from 0000 UTC 22 August 2022 to 1200 UTC 28 August versus JTWC five-day intensity forecasts (when available). Validation is relative to JTWC Working Best Track intensities [kt] along the bottom of top row with typhoon intensities indicated in red. Due to time delay for the receipt of ECEPS forecasts to JTWC, the ECEPS forecast intensities (top values in each row) are typically adjusted to begin with the JTWC intensities at T + 12 h (bottom values in each row) when there is a large difference—not adjusted for this Tokage case.

4.2. Challenges and Opportunities for TY Hinnamnor (12 W)

Wang et al. [6] highlighted STY Hinnamnor (12 W) as such a rare and unique WPAC typhoon, which we assert began in association with a long-lasting RWB event as described by Takemura and Mukougawa [8]. As indicated in Figure 3b, the early ECEPS forecasts were of a short northwestward track and recurvature. The first detection of the Hinnamnor disturbance was in the 0000 UTC 23 August ECEPS forecast, which was 5 days and 6 h before the T2TS (Table 2 (a), row 2). In Figure 5, the ten remaining ECEPS WMVN tracks are tightly clustered to 50° N. However, Hinnamnor turned westward and approached Taiwan before sharply turning poleward, and eventually passed between Korea and Japan. Unfortunately, ECEPS forecasts were not available in real time during the westward path. Consequently, the analyses here will be focused on the ECEPS predictions of Hinnamnor’s sharp turn and poleward movement (Figure 5). The most important accomplishment of the ECEPS track prediction shown in Figure 5 is the quasi-stationary period at the end of the westward track, and then the very slow poleward translation from 1 to 3 September. As indicated in Figure 2, Hinnamnor (12 W) maintained typhoon intensity during that period. Wang et al. [6] described one challenge for the Hinnamnor case as that of predicting the strong cold wake in the ocean, and how that wake would affect the intensity at the beginning of the poleward path. Wang et al. [6] also mention an eyewall replacement cycle, which is a difficult intensity forecast challenge.

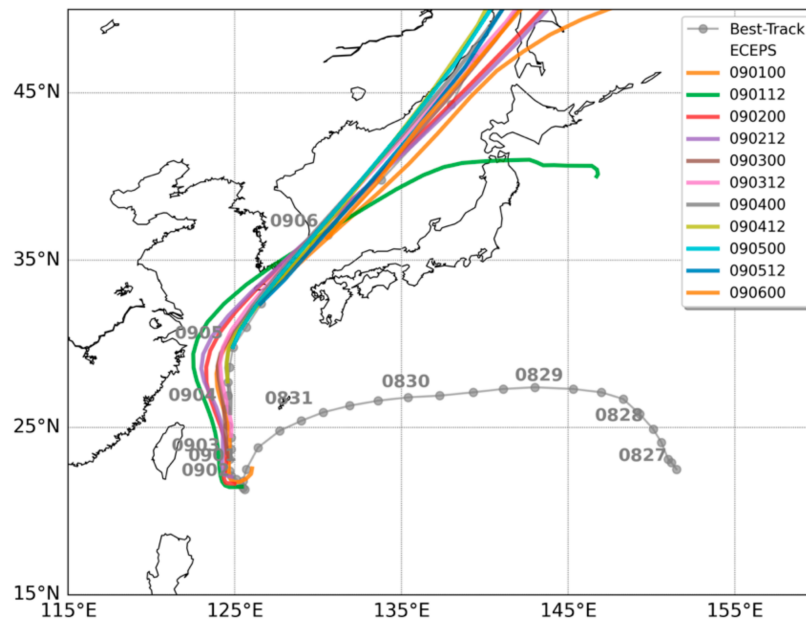


Figure 5. Weighted mean vector motion (WMVM) track forecasts as in Figure 3b for TY Hinnamnor (12 W), but including only the ECEPS forecasts for 0000 UTC 1 September to 0000 UTC 6 September.

In the ECEPS/JTWC intensity forecast validation (Figure 6), the ECEPS forecast intensities are adjusted to begin with the JTWC intensities at $T + 12$ h. Again, the focus is on the period after Hinnamnor had become quasi-stationary and then turned poleward. Note that the JTWC WBT intensity at 1200 UTC 2 September had decreased to 75 kt, which was the minimum intensity during the eyewall replacement cycle mentioned by Wang et al. [6]. The WBT intensities then steadily increased to 110 kt at 1200 UTC 4 September, and rapid decay began at 0000 UTC 6 September. In the 1200 UTC 2 September forecast (Figure 6, row 1), the ECEPS is slightly more accurate, and it provides the post-extratropical transition intensities for two days longer than the five-day JTWC forecast. This is important as Hinnamnor would be then passing close to the coast of South Korea. However, the JTWC forecast at 0000 UTC 3 September had a more accurate peak intensity period, but delayed the onset of the rapid decay period. This pattern of the ECEPS or JTWC being slightly more accurate in one forecast, and having an alternating performance in the next 12 h, characterizes the re-intensification forecasts following the minimum intensity of the Hinnamnor eyewall replacement cycle. So, the only clear advantage of the ECEPS forecasts is in the provision of intensity forecasts during the post-extratropical transition period when Hinnamnor was rapidly translating poleward through the Japan Sea. The ECEPS weighted mean intensities do provide reliable estimates of the peak winds during the cold-core extratropical transition stage, even though there was a later track forecast bifurcation after the Hinnamnor remnants passed 40° N (Figure 5).

ECEPS Date/Time	02/00		03/00		04/00		05/00		06/00		07/00		0800	
	02/12	03/12	04/12	05/12	06/12	07/12	0812							
	[90] [75]	[80] [85]	[105] [110]	[110] [100]	[75] [45]									
02/00Z (02/12Z)	75 (75)	85 94 (80) (90)	98 99 (100) (105)	106 111 (95) (85)	76 49 (70) (55)	39 37	36 30							
02/12Z (03/00Z)		80 89 (80) (90)	91 89 (100) (110)	93 94 (115) (103)	78 44 (90) (73)	35 35 (55)	35 30							
03/00Z (03/12Z)		85 (85)	95 92 (95) (105)	99 107 (105) (95)	78 50 (80) (65)	37 35 (48) (30)	38 24							
03/12Z (04/00Z)			105 104 (105) (115)	110 114 (105) (105)	76 49 (90) (75)	35 38 (60) (30)	41 36							
04/00Z (04/12Z)			110 (110)	117 121 (115) (110)	98 50 (95) (65)	37 35 (30)	31 25							
04/12Z (05/00Z)				110 122 (110) (105)	108 51 (85) (65)	39 39	38 33							
05/00Z (05/12Z)				100 (100)	45 49 (85) (60)	39 34	28 25							
05/12Z (06/00Z)					75 49 (75) (60)	39 35	34 26							

Figure 6. Validation of ECEPS and (JTWC) intensity forecasts (kt) as in Figure 4, except for Typhoon Hinnamnor (12 W) from 0000 UTC 2 September to 1200 UTC 8 September. In this case, the ECEPS forecast intensities are adjusted to begin with the JTWC intensities at T + 12 h.

4.3. Challenges and Opportunities for TY Muifa (14 W)

The spread among the ECEPS track forecasts for TY Muifa (14 W) in Figure 3c is an illustration of the extreme difficulty of forecasting some TCs during Rossby wave breaking (RWB) events. Similar to the other four typhoons and TS Talas, the pre-Muifa disturbance had a subtropical origin. As indicated in Figure 3c, the pre-Muifa (14 W) disturbance had a highly unusual track starting near 21° N, 137° E and first moving to the south before turning to the west and then having a more typical northwestward path. As Muifa slowly moved southwestward, Muifa was presumably being predicted to interact with RWB cyclonic circulations moving eastward on the poleward side of the upper-level ridge. Indeed, about 10 ECEPS forecasts in Figure 3c had false interactions leading to predictions of poleward motions and recurvature around 30° N. Thus, the development and intensification were difficult to forecast while Muifa was drifting southward when the ECEPS was predicting poleward motion toward recurvature. This is an example in which a forecaster’s close interaction with the satellite analyst would enhance the forecaster’s interpretation of the ECEPS forecasts during the early pre-formation stage.

Tan et al. (2024) [21] also utilized two ensemble models to study TY Muifa, which they referred to as a rare typhoon because it made landfall four times along the East China coast. According to the China Meteorological Administration (CMA), pre-Muifa did not form until 0000 UTC 8 September and gradually intensified into a TC at 0300 UTC 10 September. Thus, the CMA did not consider pre-Muifa to have existed during the first 15 ECEPS forecasts in Figure 3c, and only gave it the status of TS Muifa after it had been moving to the northwest for three days, according to Figure 2. While CMA designated Muifa as a typhoon in 24 h, and thus affirmed that there was an RI event following its formation, the CMA estimated that the peak intensity was 50 ms⁻¹ at 0300 UTC 11 September. By contrast, the JTWC had designated Muifa as a TS already at 0000 UTC 7 September and a TY at 1800 UTC 9 September (Table 1, row 3). Furthermore, the JTWC peak intensity was 115 kt at 0000 UTC 11 September. Given these differences in the CMA and JTWC intensities and

their timings, it would be difficult to compare the ECEPS forecasts with the Tan et al. [21] ensemble forecasts, which were entirely focused on 5-day forecasts of the four landfalls (see Figure 2).

While the pre-Muifa disturbance first appeared in the 1200 UTC 31 August ECEPS forecast, it was not until 1200 UTC 4 September that pre-Muifa was indicated in the JTWC WBT (Table 1, row 3). Even at 0000 UTC 8 September, when Muifa had reached its southernmost point, and a northwestward track was the correct forecast, the ECEPS was not predicting favorable conditions for the rapid intensification of Muifa. While Muifa intensified from 35 kt at 1200 UTC 7 September to 115 kt at 0000 UTC 11 September (80 kt in 84 h), the ECEPS was correctly predicting a non-occurrence of an RI event following formation (Table 2, row 3). Whereas the ECEPS was predicting TS Muifa would not become a TY until 42 h after formation, Muifa actually took 66 h to become a TY (Table 2 (b), row 3). However, Muifa then increased 50 kt in 30 h to the peak intensity of 115 kt, but the ECEPS continued to only predict slow intensification and missed this large RI event. The tentative conclusion is that the ECEPS can predict the environmental conditions for T2TS and even T2TY when they occur (Table 2 (b)), but the ECEPS model's physics are not capable of predicting the inner-core spin-up rate that exists when a small inner-core vortex is undergoing very rapid intensification. A second contributor is that the ECEPS initialization does not include the TC Vitals. That is, if the satellite analyst had documented in the TC Vitals that the TC vortex structure had already become better organized and had rapidly intensified during the 12 h since the prior intensification, this information would not be included in the ECEPS initialization.

Thus, the focus of the validation of the ECEPS intensity forecasts for TY Muifa (14 W) shown in Figure 7 is on after the period of maximum intensity and when Muifa is making multiple landfalls [21] and rapidly decaying. As indicated in the JTWC WBT (Figure 7, top row), the intensities are between 80 kt and 90 kt during the approach to the first landfall at 1230 UTC 14 September [21]. If the ECEPS intensity forecasts at $T + 12$ h are adjusted to begin with the JTWC intensities at that time, the ECEPS intensities are within fixed uncertainties leading up to that first landfall. The ECEPS intensities during the first landfall tend to be higher than the JTWC intensities, but that may just be because the ECEPS track forecast appears to be slightly farther offshore [see Figure 3]. While the advantage of the ECEPS forecasts is that they provide intensity guidance for longer periods than the JTWC 5-day forecasts, these ECEPS intensities quickly decay to values < 20 kt.

ECEPS Date/Time	12/00		13/00		14/00		15/00		16/00		17/00		18/00	
	12/12	13/12	14/12	15/12	11/12	17/12	18/12							
	[80]	[85]	[90]	[85]	[85]	[80]	[60]	[40]	[30]	[20]				
12/00Z (12/12z)	80	85 (85)	82 (80)	78 (75)	79 (70)	79 (65)	61 (53)	42 (40)	35 (30)	16 (20)	14	13	19	26
12/12Z (13/00Z)		85	90 (90)	89 (90)	93 (85)	88 (70)	65 (50)	54 (40)	19 (30)	12 (25)	10	8	21	
13/00Z (13/12Z)			90	85 (90)	95 (85)	87 (70)	73 (45)	54 (35)	19 (28)	14 (20)	12	10	20	
13/12Z (14/00Z)				85	85 (85)	89 (75)	70 (50)	55 (35)	27 (30)	24 (25)	21	14	20	20
14/00Z (14/12Z)					85	80 (80)	61 (60)	32 (45)	33 (35)	28 (30)	18 (25)	17 (20)	17	26
14/12Z (15/00Z)						80	60 (60)	61 (45)	33 (35)	30 (30)	18 (20)	17	17	26
15/00Z (15/12Z)							60	59 (40)	33 (35)	30 (30)	15 (20)	18	21	29
15/12Z (16/00Z)								40	39 (30)	34 (20)	18 (20)	21	25	34

Figure 7. Validation of ECEPS and (JTWC) intensity forecasts (kt) as in Figure 4, except for Typhoon Muifa (14 W) from 0000 UTC 12 September to 1200 UTC 18 September. In this case, the ECEPS forecast intensities are adjusted to begin with the JTWC intensities at T + 12 h.

4.4. Challenges and Opportunities for TY Merbok (15 W)

At 0600 ITC 10 September when Muifa (14 W) was rapidly intensifying southeast of Taiwan to a peak intensity of 115 kt, JTWC began tracking Tropical Depression Merbok (15 W) far to the east near 21° N, 158° E (Figure 2). The first detection of the pre-Merbok disturbance in the ECEPS in Figure 3d was at 1200 UTC 4 September (early detection by 3.75 days), but this was seven days before JTWC designated Merbok as a TS (Table 2 (a), row 4). Merbok continued to intensify slowly, became a TY at 1800 UTC 13 September, and reached its peak intensity of 70 kt at 0600 UTC 14 September. Another forecasting challenge with Merbok was that at the last WBT of 1800 UTC 15 September, the intensity was still 55 kt, and Merbok was moving rapidly toward 50° N, 170° E.

The intensity validation for the ECEPS forecasts of Merbok in Figure 8 include both the intensification stage beyond 35 kt and the decay stage. In this case, no adjustments were made to ECEPS intensities to start from the T + 12 h JTWC intensities. As indicated in Table 2 (b) (row 4), there was no RI event following the first time the Merbok intensity became 35 kt (1200 UTC 11 September), and the ECEPS had correctly predicted that slow intensification. However, the JTWC WBT did not indicate TY intensity for Merbok until 0000 UTC 14 September (Figure 8, top row). By contrast, the ECEPS forecast from 1200 UTC 11 September had an RI event of 35 kt at 0000 UTC 12 September to 66 kt at 0000 UTC 13 September, and a continued intensification to a peak intensity of 92 kt at 1200 UTC 14 September (Figure 8, first row). Similarly, the JTWC forecast had a faster intensification to a peak intensity of 85 kt at 0000 UTC 14 September (Figure 8, first row bottom), which is 20 kt higher than the peak intensity in the JTWC WBT. Both the ECEPS forecast and the JTWC forecast start the decay stage at the same time (0000 UTC 15 September). Whereas that JTWC forecast terminates Merbok with an intensity of 28 kt at 1200 UTC 16 September, the ECEPS predicts an extratropical transition (WCM < 0, cold-core) intensity of 57 kt at 1200 UTC 15 September with sustained winds near 50 kt for another 48 h.

ECEPS Date/Time	12/00 12/12		13/00 13/12		14/00 14/12		15/00 15/12		16/00 16/12		17/00 17/12		18/00 18/12	
	[35]	[45]	[55]	[60]	[65]	[65]	[65]	[55]						
11/12Z (12/00Z)	35 (35)	52 (40)	66 (50)	72 (65)	83 (85)	92 (85)	73 (80)	57 (70)	55 (55)	50 (28)	46	47	36	27
12/00Z (12/12Z)	35	45 (45)	54 (55)	58 (65)	67 (70)	75 (75)	66 (80)	56 (85)	55 (70)	50 (55)	49	49 (30)	32	23
12/12Z (13/00Z)		45	55 (55)	62 (65)	73 (75)	83 (85)	66 (80)	79 (75)	52 (65)	45 (33)	51	62	50	24
13/00Z (13/12Z)			55	60 (60)	69 (70)	77 (75)	77 (85)	85 (80)	54 (70)	47 (60)	53 (30)	97	64	29
13/12Z (14/00Z)				60	65 (65)	73 (70)	64 (75)	54 (80)	54 (40)	51	78	109	88	62
14/00Z (14/12Z)					65	70 (65)	76 (75)	86 (80)	56 (70)	50	96	115	100	88
14/12Z (15/00Z)							65 (65)	65 (65)	55 (60)	49	84	106	89	85

Figure 8. Validation of ECEPS and (JTWC) intensity forecasts (kt) as in Figure 4, except for Typhoon Merbok (15 W) from 0000 UTC 12 September to 1200 UTC 18 September. In this case, no adjustment of the ECEPS forecast to begin with the JTWC intensities at T + 12 h is applied.

This intensification pattern of both ECEPS and JTWC predicting higher peak intensities than the JTWC WBT peak intensity of 65 kt continues for the rest of the forecasts in Figure 8. Similarly, the decay stage begins at about the same time for both ECEPS and JTWC forecasts. Each of the JTWC decay stage forecasts terminates with a rapid decay in the last 12 h of the 5-day forecast. By contrast, the ECEPS decay stage forecast is for an extratropical transition with persistent high winds.

The most intriguing aspect of the ECEPS forecasts for post-Merbok is that starting with the 0000 UTC 13 September forecast, a transition to an extremely intense, warm-core vortex is predicted (Figure 8, rows 5–8). In each of these ECEPS forecasts, the peak intensity is predicted to be at 1200 UTC 17 September. Note that the JTWC forecasts from 1200 UTC 14 September and 0000 UTC 15 September end at 70 kt and 60 kt, respectively (Figure 8, rows 6 and 7), and JTWC did provide some track forecasts toward the Aleutian Islands.

A take-away from these ECEPS forecasts for Merbok is that when the TC intensity is being predicted to be sustained at Category 3 or more, a recalibration of the WCM–intensity relationship is needed. Certainly, any ECEPS prediction of a post-extratropical transition storm becoming warm-core as in this Merbok case needs to be recalibrated.

4.5. Challenges and Opportunities for TY Nanmadol (16 W)

Not only did the JTWC begin issuing advisories on pre-Merbok in the eastern region of the domain while TY Muifa (14 W) was undergoing RI southeast of Taiwan, the JTWC, at 0000 UTC 11 September, began issuing advisories on pre-Nanmadol (16 W) starting at almost the identical location as Muifa began (Figure 2). According to JTWC, pre-Nanmadol did not become a TD until 1200 UTC 12 September and did not become a TS until 1800 UTC 13 September (Table 2 (a), row 5). Although Nanmadol was listed in Table 2 (b) (row 5) as maybe having a rapid intensification immediately following formation, the actual RI event followed the T2TY with an intensification to a peak intensity of 135 kt at 1800 UTC 16 September (70 kt in 30 h).

The ECEPS provided accurate guidance for pre-Nanmadol, with early detection 7.0 days prior to T2TS and 8 days and 6 h prior to T2TY (Table 2 (a), row 5). The first three ECEPS track forecasts exaggerated the initial east-northeast motion (Figure 3c), but then

predicted well the quasi-stationary period. The northwestward track spread was quite small until it neared recurvature following landfall on southern Japan (Figure 2). Recall that the review by Conroy et al. [1] had provided the Nanmadol (16 W) track as a challenge for the TC forecaster community, and Figure 3c indicates that the ECEPS is up for that track forecast challenge.

However, the ECEPS failed to predict the slow intensification rate from T2TS to T2TY, and especially failed to predict the rapid intensification following the T2TY. In the 1200 UTC 13 September ECEPS forecast, the peak intensity forecast was 140 kt, but it was not predicted until 1200 UTC 18 September, which was 48 h late. As indicated for the failed TY Muifa (14 W) ECEPS rapid intensification forecasts, the first conclusion is that the ECEPS model physics are not capable of predicting the inner-core spin-up rates when a small inner-core vortex is undergoing very RI. A second contributor is that the ECEPS initialization does not include the TC Vitals.

Thus, the focus of the validation of the ECEPS intensity forecasts for TY Nanmadol (16 W) in Figure 9 is on the decay stage. While the 1200 UTC ECEPS intensity forecast did not seem to need an adjustment to the T + 12 h JTWC intensity, the following ECEPS forecasts did need that adjustment. As in the Muifa case, both the ECEPS and the JTWC intensity forecasts maintain intensities higher than the verifying JTWC WBT intensities, and thus do not decay as soon, or as rapidly, as the WBT decay rates. As indicated in Figure 3f, the ECEPS track forecasts were just offshore rather than on the landfall track in Figure 2. After that first landfall, the ECEPS intensity decay rates and the JTWC decay rates (when available within the 5-day period) agree quite well, which may be because both ECEPS and JTWC have track forecasts just offshore as in Figure 2.

ECEPS Date/Time	17/00		18/00		19/00		20/00		21/00		22/00		23/00	
	17/12	17/12	18/12	18/12	19/12	19/12	20/12	20/12	21/12	21/12	22/12	22/12	23/12	23/12
	[130]	[125]	[105]	[80]	[60]	[50]	[40]							
16/12Z (17/00z)	115 (130)	126 (125)	135 (120)	136 (105)	128 (90)	114 (75)	97 (60)	64 (50)	36 (40)	33 (38)	33 (35)	31	32	30
17/00Z (17/12Z)	130	125 (125)	136 (120)	138 (85)	124 (75)	97 (60)	47 (53)	36 (45)	40 (40)	34 (35)	30	30	31	34
17/12Z (18/00Z)		125	105 (105)	100 (90)	85 (75)	66 (60)	67 (50)	38 (43)	38 (35)	36 (33)	36 (30)	49	43	
18/00Z (18/12Z)			105	80 (80)	57 (65)	21 (55)	39 (45)	36 (40)	33 (38)	33 (35)	32			
18/12Z (19/00Z)				80	60 (60)	48 (50)	37 (40)	34 (35)	30	27				

Figure 9. Validation of ECEPS and (JTWC) intensity forecasts (kt) as in Figure 4, except for Typhoon Nanmadol (16 W) from 0000 UTC 17 September to 1200 UTC 23 September. In this case, no adjustment to the T + 12 h JTWC intensity is made for the first ECEPS forecast, but it is made for the later ECEPS forecasts.

4.6. Challenges and Opportunities for TS Talas (17 W)

Whereas the first JTWC Invest for TS Talas was at 0000 UTC 20 September, the first detection in the ECEPS, shown in Figure 3f, of the pre-Talas disturbance was at 0000 UTC 14 September (early detection by 6.0 days). This information for TS Talas (17 W) does not appear in Table 2 (a) because according to the JTWC WBT, the peak intensity of Talas was 35 kt for only one time (0000 UTC 23 September). According to the JTWC WBT, pre-Talas on 21 September passed just to the east of where Nanmadol had become a TS at 1800 UTC 13 September. Talas continued to move poleward E and became TD Talas near 25.4° N, 138.9° E. The subsequent track to the northeast parallel to the southern coast of mainland Japan (Figure 2) is indicative of the potential threat if Talas had continued to intensify.

Validation for Talas (17 W) in Figure 10 includes only the ECEPS intensity forecasts as JTWC was not issuing official forecasts for pre-Talas, which was so weak, and presumably was not expected to become a TS. Consequently, a series of 16 ECEPS intensity forecasts every 12 h from 0000 UTC 16 September to 1200 UTC 23 September can be validated, which started four days before the first JTWC WBT intensity and extended 24 h after the last WBT intensity. In those first two ECEPS intensity forecasts on 16 September, pre-Talas was predicted to begin in about 3 days as a warm-core disturbance and have peak intensities of 44 kt and 58 kt, respectively. However, Talas was predicted to then become cold-core, with peak winds of 29–35 kt. In the ECEPS forecast from 17 September, Talas was predicted to start cold-core on 19 September, become warm-core for three days, and then again finish cold-core. From 0000 UTC 18 September onward, Talas was predicted to be cold-core, with the exceptions being the first two times in the 1200 UTC 18 September forecast and the first six times in the 0000 UTC 19 September forecast. While the early ECEPS WCM predictions of a potential TY were incorrect, the subsequent predictions that the disturbance was a cold-core subtropical cyclone would have assisted the JTWC in analyzing the intensity from satellite imagery. The ECEPS weighted mean intensities also provide helpful estimates of the peak winds during the cold-core, subtropical cyclone stages of Talas (17 W).

ECEPS Date/Time	19/00 19/12		20/00 20/12		21/00 21/12		22/00 22/12		23/00 23/12		24/00 24/12		25/00 25/12	
			[15]	[20]	[20]	[20]	[30]	[30]	[35]	[25]	[20]	[15]		
16/00Z 16/12Z		36	40 43 44 48		38 44 46 40		42 43 39 47		24 26 44 58		26 24 53 34		26 33 37 36	
17/00Z 17/12Z	17 22	22 21	26 28 24 26		26 37 27 31		42 45 30 31		48 27 28 28		29 26 25 26		28 26 27 26	
18/00Z 18/12Z	21 23		24 25 31 29		23 24 23 24		25 27 25 25		28 25 25 24		25 26 24 27		28 32 28 27	
19/00Z 19/12Z			26 29 24 24		25 24 24 24		24 25 25 25		26 26 24 24		26 27 19 17		28 26	
20/00Z 20/12Z			24 (Missing)		23 23		24 24		24 23		22 26		27 24	
21/00Z 21/12Z					26 25 26		28 33 27 28		27 27 26 26		22 22 22 23		25 24 25 21	
22/00Z 22/12Z							(Missing) 29		29 31		24 26		21 20	
23/00Z 23/12Z									(Missing) 28		24 24		24 19	

Figure 10. Validation of only the ECEPS intensity forecasts each 12 h from 0000 UTC 16 September to 1200 UTC 23 September versus JTWC Working Best Track intensities from 0000 UTC 20 September to 0000 UTC 22 September in brackets in top row. In this table, the warm-core TC intensities are in black and the cold-core intensities are in blue.

5. Summary and Discussion

The primary objective of this article in the *Special Issue on Typhoon/Hurricane Dynamics and Prediction* was to document the performance of the ECEPS in predicting the lifecycle of the six tropical cyclones that formed during the long-lasting RWB event. Two of these six TCs (Hinnamnör—12 W, and Nanmadol—16 W) had been cited in the literature as examples of difficult, challenging TCs to predict. While we do not calculate the 300 K potential vorticity composites during August–September 2022 when the six TCs existed that were similar to the Takemura and Mukougawa [9] composites, the six TC tracks in

Figure 2 have similar track characteristics to those in Figure 1. Specifically, all six TCs start between 20° N and 25° N, with three starting between 150° E and 160° E and a tight cluster of three starting between 136° E and 139° E. All five typhoons recurved north of 30° N, and the three typhoons that did not make landfall had long tracks to 50° N and beyond (Figure 2).

As in our previous studies with the ECEPS, the objectives were to provide earlier, pre-formation track and intensity forecasts, and longer track and intensity forecasts of up to 14 days, which in many cases include the decay stage and even the post-extratropical transition stage. Thus, the six TC track forecast summaries in Figure 3 include as many as thirty 12 h ECEPS forecasts. Using the track forecast spread as a measure of uncertainty, a key factor was the ECEPS's capability to predict the initial position. For Tokage (11 W), Hinnamnor (12 W), and Nanmadol (16 W) the small initial position uncertainties led to relatively smaller track forecast spreads (Figure 3a,b,e, respectively). By contrast, the initial position uncertainties for Merbok (Figure 3d) and for Talas (Figure 3f) were major contributors to the track forecast spreads. The extremely large track forecast spread for Muifa (Figure 3c) is attributed to the ECEPS over-predicting the pre-formation intensity of the pre-Muifa disturbance. Presumably, the satellite analysts were accurately monitoring the intensity of the pre-Muifa disturbance, as the JTWC did not start the WBT until 1200 UTC 4 September (Table 1, row 3), and the Chinese Meteorological Association did not indicate that pre-Muifa forming until 8 September [21]. If Figure 3c only included the ECEPS track forecasts after 8 September (i.e., omitting the first 15 forecasts), the track forecast spread would be much smaller, as in the other track forecasts in Figure 3.

Validations of the ECEPS intensity forecasts relative to the JTWC WBT intensities (when available) for each of the six TCs are given in Figures 4 and 6–10. Due to the almost 12 h delay before the ECEPS files are available at JTWC, it is the ECEPS T + 12 h and beyond intensity forecast that is comparable with the corresponding JTWC intensity forecast. The purpose is to demonstrate that the ECEPS forecast could provide earlier (pre-formation) and/or extended (up to 14 days) guidance. The key result for Tokage (11 W) is that from the time of the first JTWC forecast at 1200 UTC 22 August, the ECEPS forecasts of the intensification to a peak intensity of 100 kt, and then a rapid decay as a cold-core cyclone, are generally quite good. The focus of the ECEPS's intensity validation for Hinnamnor (12 W) had to be restricted to the period after it had become quasi-stationary southeast of Taiwan, and then turned poleward, and later passed along the South Korean coast. If these later ECEPS intensity forecasts were adjusted to begin with the JTWC T + 12 h intensity, the ECEPS intensity forecasts and the JTWC forecasts were both accurate. So, the only clear advantage of the ECEPS forecasts was in providing intensity forecasts during the post-extratropical transition period when Hinnamnor was rapidly translating poleward through the Japan Sea.

Due to the pre-formation stage ECEPS forecasts over-predicting the Muifa (14 W) intensity that resulted in the early and fictitious track forecast spreads in Figure 3c, it is somewhat difficult to validate the later "real" intensification stage. The ECEPS also over-predicted the relatively slow intensification from T2TS to T2TY, but then under-predicted the large RI after the T2TY. Thus, the focus of the validation of the ECEPS intensity forecasts for Muifa (14 W) was after the period of maximum intensity and it was making multiple landfalls along the East China coast. The key advantage of the ECEPS in this case was that intensity guidance was provided for longer periods than the JTWC 5-day forecast, which would be important for disaster preparations in advance of the landfalls along the East China coast.

The intensity validation for the ECEPS intensity forecasts for Merbok (15 W) included both the intensification stage beyond 35 kt and the decay stage. The ECEPS forecast and the JTWC forecast both predicted well the intensification stage with somewhat higher peak intensities than in the JTWC WBT. The most intriguing aspect of the ECEPS forecasts for post-Merbok was predicting a transition to an intense, warm-core vortex after Merbok had moved beyond 50° N and headed toward the Aleutian Islands.

The ECEPS provided accurate guidance for pre-Nanmadol (16 W) with early detection 7.0 days prior to T2TS and 8 days and 6 h prior to T2TY. The ECEPS over-predicted the slow intensification rate from T2TS to T2TY, but then failed to predict the large intensification following the T2TY. The tentative conclusion is that the ECEPS model physics are not capable of predicting the inner-core spin-up rates when a small inner-core vortex is undergoing large RI. A second contributor is that the ECEPS initialization does not include the TC Vitals, so when the TC intensity has been increasing beyond what the ECEPS has been predicting, that will not be the starting intensity in the ECEPS forecast.

Validation for Talas (17 W) included only the ECEPS's intensity forecasts as JTWC was not issuing forecasts for pre-Talas, which was so weak. Whereas the early pre-Talas ECEPS predictions were of it being warm-core with intensities as high as 58 kt, later forecasts consistently predicted that Talas was a cold-core, subtropical cyclone that would not pose a threat to the Japanese mainland.

Wang et al. [6] make a strong case that Hinnamnor (12 W) would be an excellent case for in-depth mechanistic studies of typhoon tracks, intensity, and structural changes with different numerical models. We concur, and advocate that all six TCs that occurred during this long-lasting RWB event should also be included in these studies. TY Muifa (14 W) would have had a strong interaction with the cold ocean wake of Hinnamnor, and both TY Nanmadol (16 W) and TS Talas (17 W) crossed that cold wake. Many artificial intelligence (AI) articles are proposing machine learning-based methods as an alternative to traditional numerical weather prediction models. For example, Lam et al. (2023) [22] describe their GraphCast technique for skillful medium-range global weather forecasting that has been trained directly from reanalysis data to predict in under 1 min hundreds of weather variables, including TC tracking. The obvious question is whether GraphCast can predict the track of Hinnamnor, which started at an unusual position, turned to the west rather than recurving as Tokage (11 W) did, moved rapidly westward at TY intensity, suddenly turned to the south, became quasi-stationary, and then moved poleward to undergo extratropical transition over the Japan Sea (Figure 2). Similar questions could be asked for the other four TYs. Furthermore, can GraphCast predict the timing, locations, and magnitudes of the RI events?

Another intriguing question regarding the five typhoons that all recurved is what are the downstream impacts? Recall that TY Merbok (15 W) propagated rapidly to 40° N and was still a TS as it approached 50° N (Figure 2). The ECEPS predicted that Muifa would undergo extratropical transition, but would later re-develop as a warm-core cyclone as it approached the Aleutian Islands. TY Tokage (11 W) had earlier propagated rapidly to 50° N, and the ending-TY stage of Hinnamnor (12 W) was at 40° N. What, then, are the downstream impacts of such TY stage outflows at such high latitudes?

Other questions related to this RWB event should also be explored to provide the context for the development of the six TCs. What dynamic factors led to such a strong and long-lasting RWB event? What environmental factors allowed these six TCs to become so intense and led to all of them recurving? Will similar RWB events with multiple TCs and subtropical cyclones become more common in global climate change scenarios?

Author Contributions: Conceptualization: R.L.E. and H.-C.T. have together published journal articles since 2014 on the ensemble storm weighted mean vector motion (WMVM) track forecasts, and H.-C.T. and R.L.E. have jointly over five years developed the combined Weighted Analog Intensity Prediction (Pacific), and T.P.M. conceived and developed the tropical cyclone vortex tracker. Methodology: H.-C.T. and R.L.E. have jointly conceived the methodology of warm-core magnitude (WCM) with the assistance of T.P.M.; software coding for warm-core magnitude has been done by H.-C.T. and W.-C.C., and T.P.M. has continued to upgrade the vortex tracker code. Validation: R.L.E. and H.-C.T. have jointly conceived the validation technique. Writing, R.L.E. and H.-C.T. have been responsible for the text, and H.-C.T. and W.-C.C. have been responsible for creating the figures. All authors have read and agreed to the published version of the manuscript.

Funding: R.L.E. and H.-C.T. had a two-year Joint Hurricane Testbed grant from the NOAA OAR Office of Weather and Air Quality (OWAQ); R.L.E. is also funded by the Office of Naval Research

Grant N00014-19-1-2465. H.-C.T. is supported by the Taiwan National Science and Technology Council (NSTC 112-2625-M-032-001). T.P.M.'s participation was internally funded at the Geophysical Fluid Dynamics Laboratory.

Institutional Review Board Statement: Not applicable.

Informed Consent Statement: Not applicable.

Data Availability Statement: JTWC best tracks can be downloaded at <https://www.metoc.navy.mil/jtwc/jtwc.html?western-pacific> (accessed on 1 March 2024).

Acknowledgments: Penny Jones is thanked for her excellent contributions to the preparation of the manuscript.

Conflicts of Interest: The authors declare no conflicts of interest. The funders had no role in the design of the study, the analyses or interpretation of the data, in the writing of the manuscript, or in the decision to publish the results.

References

- Conroy, A.; Titley, H.; Rivett, R.; Feng, X.; Methxen, J.; Hodges, K.; Bammer, A.; Burton, A.; Chakraborty, P.; Chen, G.; et al. Track forecast: Operational capacity and new technologies—Summary from the Tenth International Workshop on Tropical Cyclones (IWTC-10). *Trop. Cyclone Res. Rev.* **2023**, *12*, 64–80. [[CrossRef](#)]
- Sampson, C.R.; Schrader, A.J. The automated tropical cyclone forecasting system (version 3.2). *Bull. Amer. Meteorol. Soc.* **2000**, *81*, 1131–1140. [[CrossRef](#)]
- Schreck, C.J.; Vitart, F.; Camargo, S.J.; Camp, J.; Darlow, J.; Elsberry, R.; Gottschalck, J.; Gregory, P.; Hansen, K.; Jackson, J.; et al. Advances in tropical cyclone prediction on subseasonal time scales during 2019–2022. *Trop. Cyclone Res. Rev.* **2023**, *12*, 136–150. [[CrossRef](#)]
- Elsberry, R.L.; Tsai, H.-C.; Capalbo, C.; Chin, W.-C.; Marchok, T.P. Opportunity for tropical cyclone lifecycle predictions from pre-formation to ending stage: Eastern North Pacific 2021 season. *Atmosphere* **2022**, *13*, 1008. [[CrossRef](#)]
- Wadler, J.B.; Rudzin, J.E.; Jaimes, B.; Chen, J.; Fischer, M.; Chen, G.-H.; Qin, N.; Tang, B.; Li, Q.-Q. A review of recent research progress on the effect of external influences on tropical cyclone intensity change. *Trop. Cyclone Res. Rev.* **2023**, *12*, 2000–2015. [[CrossRef](#)]
- Wang, Q.; Zhao, D.J.; Duan, Y.H.; Guan, S.D.; Dong, L.; Xu, H.X.; Wang, H. Super Typhoon Hinnamor (2022) with a record-breaking life span over the western North Pacific. *Adv. Atmos. Sci.* **2023**, *40*, 1558–1566. [[CrossRef](#)]
- Enomoto, T.; Hoskins, B.J.; Matsuda, Y. The formation mechanism of the Bonin high in August. *Q. J. R. Meteorol. Soc.* **2023**, *129*, 157–178. [[CrossRef](#)]
- Takemura, K.; Kubo, Y.; Maeda, S. *Relation between a Rossby Wave-Breaking Event and Enhanced Convective Activities in August 2016*; SOLA: Tokyo Japan, 2017; pp. 120–124.
- Takemura, K.; Mukougawa, H. Dynamical relationship between quasi-stationary Rossby wave propagation along the Asian jet and Pacific-Japan pattern in boreal summer. *J. Meteor. Soc. Japan* **2020**, *98*, 169–187. [[CrossRef](#)]
- Fudeyasu, H.; Yoshida, R. Statistical analysis of the relationship between upper-tropospheric cold lows and tropical cyclone genesis over the western North Pacific. *J. Meteor. Soc. Japan* **2020**, *97*, 439–451. [[CrossRef](#)]
- Gelarneau, T.J.; McTaggart-Cowan, R.; Bosart, L.F.; Davis, C.A. Development of North Atlantic tropical disturbances near upper-level potential vorticity streamers. *J. Atmos. Sci.* **2015**, *72*, 572–597. [[CrossRef](#)]
- Papin, P.P.; Bosart, L.F.; Torn, D.R. A feature-based approach to classifying summer time potential vorticity streamers linked to Rossby wave breaking in the North Atlantic basin. *J. Clim.* **2020**, *39*, 5953–5969. [[CrossRef](#)]
- Zhang, G.; Wang, Z.; Dunkerton, T.J.; Peng, M.S.; Magnusdottir, G. Characteristics and impacts of extratropical Rossby wave breaking during the Atlantic hurricane season. *J. Clim.* **2017**, *30*, 2362–2379. [[CrossRef](#)]
- Li, W.; Wang, Z.; Zheng, G.; Peng, M.S.; Benjamin, S.G.; Zhao, M. Subseasonal variability of Rossby wave breaking and impacts on tropical cyclones during the North Atlantic warm season. *J. Clim.* **2018**, *31*, 9679–9695. [[CrossRef](#)]
- Marchok, T. Important factors in tracking of tropical cyclones in operational models. *J. Appl. Meteor. Climatol.* **2021**, *60*, 1265–1284. [[CrossRef](#)]
- Tsai, H.-C.; Elsberry, R.L.; Chin, W.-C.; Marchok, T.P. Opportunity for early warnings of Typhoon Lekima from two global ensemble model forecasts of formation with 7-day intensities along medium-range tracks. *Atmosphere* **2020**, *11*, 1162. [[CrossRef](#)]
- Elsberry, R.L.; Tsai, H.-C.; Chin, W.-C.; Marchok, T.P. Advanced global model ensemble forecasts of tropical cyclone formation, and intensity predictions along medium-range tracks. *Atmosphere* **2020**, *11*, 1002. [[CrossRef](#)]
- Elsberry, R.L.; Tsai, H.-C.; Chin, W.-C.; Marchok, T.P. Predicting rapid intensification events following tropical cyclone formation in the western North Pacific based on ECMWF ensemble warm core evolutions. *Atmosphere* **2021**, *12*, 847. [[CrossRef](#)]
- Elsberry, R.L.; Tsai, H.-C.; Capalbo, C.; Chin, W.-C.; Marchok, T.P. Critical pre-formation decision flowchart to apply tropical cyclone lifecycle predictions in eastern North Pacific. *Atmosphere* **2023**, *14*, 616. [[CrossRef](#)]

20. Elsberry, R.L.; Tsai, H.-C.; Marchok, T.P.; Feldmeier, J.W.; Chen, H.-J.; Velden, C.S. Future opportunities with WPAC tropical cyclone lifecycle predictions. In Proceedings of the 2023 PACOM Tropical Cyclone Conference, Honolulu, HI, USA, 28–30 March 2023.
21. Tan, Y.; Huang, W.; Zhang, X. Assessment and ensemble-based analysis of the landfalling Typhoon Muiff (2022). *Atmosphere* **2024**, *15*, 343. [[CrossRef](#)]
22. Lam, R.; Sanchez-Gonzalez, A.; Willson, M.; Wirnsberger, P.; Fortunato, M.; Alet, F.; Ravuri, S.; Ewalds, T.; Eaton-Rosen, Z.; Hu, W.; et al. Learning skillful medium-range global weather forecasting. *Science* **2023**, *382*, 1416–1421. [[CrossRef](#)] [[PubMed](#)]

Disclaimer/Publisher’s Note: The statements, opinions and data contained in all publications are solely those of the individual author(s) and contributor(s) and not of MDPI and/or the editor(s). MDPI and/or the editor(s) disclaim responsibility for any injury to people or property resulting from any ideas, methods, instructions or products referred to in the content.